Analytical Determination of Shape Factors from a Surface Element to an Axisymmetric Surface

S. J. Morizumi*
TRW Space Technology Laboratories, Redondo Beach, Calif.

I. Introduction

In the prediction of radiant heat rates from an exhaust plume (gaseous or particle) to a spacecraft, an equivalent surface radiation technique may be used. In the use of such a technique, it is important that the shape factor from a surface point of the spacecraft to its exhaust plume be known. Thus, to facilitate studies of radiative heat transfer between a spacecraft and its engine exhaust plume, an analytical method of determining shape factor is desired. Presented herein is the development of such a technique that calculates the shape factor between a surface element and an axisymmetric surface. The analysis is based on Nusselt's double-projection principle, which is described in Ref. 1. The technique is considered extremely useful since it requires no physical model nor optical equipment. It is also readily adaptable to a computer program.

II. Analytical Solutions

The analytical solution of the shape factor for a paraboloidal surface is developed initially. This solution is also applicable to a conical and a cylindrical surface by simplification.

In the development of the solutions, a right-handed rectangular coordinate system is selected at the normal projection point of a surface element on the centerline of an axisymmetric surface. The x axis is directed along the surface centerline, and the y axis is pointed toward the surface element.

A. *Shape factor to paraboloidal surface (see Fig. 1)*

Let the equation defining the shape of a paraboloidal surface be

$$R = \mu + \nu x + \xi x^2 \tag{1}$$

If a surface element at a point P ($x = 0, y = \rho, z = 0$) is considered such that its normal unit vector $\mathbf{n}$ lies in the x-y plane at an angle γ_0 with respect to the y axis, the surface element sees only a portion of the paraboloidal surface which is unshaded from the element. It is seen that the surface element can see only the surface downrange of $\gamma = \gamma_0$. Furthermore, the element sees only a portion of the surface where the normal vector $\mathbf{N}$ is at an angle equal to or less than 90° with respect to a line joining the point P with a point on the surface. This condition is expressed by the following vector relation:

$$-\mathbf{L}\cdot\mathbf{N} \geq 0$$

The substitution of the vector expressions for $\mathbf{L}$ and $\mathbf{N}$ into the foregoing relation results in

$$\sin\phi \geq (1/\rho)(\mu - \xi x^2)$$

This relation implies that there is a minimum angle ϕ_m that defines the boundary of a visible region of the surface. Thus, the visible region of the paraboloidal surface is bounded by the following relations:

$$\gamma \leq \gamma_0 \tag{2a}$$

$$\sin\phi \geq \sin\phi_m = (\mu - \xi x^2)/\rho \tag{2b}$$

If a view-plane from P with a view angle γ is considered (see Fig. 1), the intersections of this plane with the boundary curves of (2b) yield

$$h = R\sin\phi_m = (R/\rho)(\mu - \xi x^2) \tag{3}$$

$$\tan\gamma = (\rho - h)/x \tag{4}$$

$$\left(\frac{S}{l}\right) = \left(\frac{R}{\rho}\right)\left\{\frac{1 - (h/R)^2}{[1 - (h/\rho)]^2 + (x/\rho)^2}\right\}^{1/2} \tag{5}$$

Using the double-projection principle,[1] the shape factor between the surface element P and the paraboloidal surface is obtained by projecting the boundary curves [Eq. (2b)] on the surface of the hemisphere constructed around the point P and then down to the base of the hemisphere, which is in the plane of the surface element.

The intersection of the surface of the hemisphere with the triangle formed by the two intersection points B and C and the point P results in the following geometric relations (see Fig. 2):

$$\lambda = \frac{R_0(S/l)}{[1 + (S/l)^2]^{1/2}} \tag{6}$$

$$\eta = \frac{R_0\cos(\gamma_0 - \gamma)}{[1 + (S/l)^2]^{1/2}} \tag{7}$$

It is observed from Fig. 2 that the double-projection of a line segment BC on the base of the hemisphere is an elliptical arc segment KJ. If these projections are integrated between two limiting view angles, the projection of the paraboloidal surface on the base of the hemisphere between these two angles is obtained. If, however, a line segment KJ instead of the

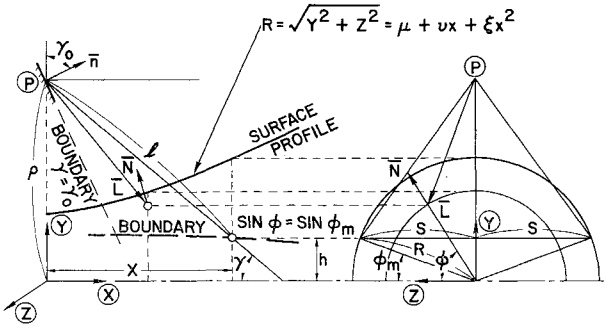

Fig. 1 Geometric relationship between surface element and paraboloidal surface.

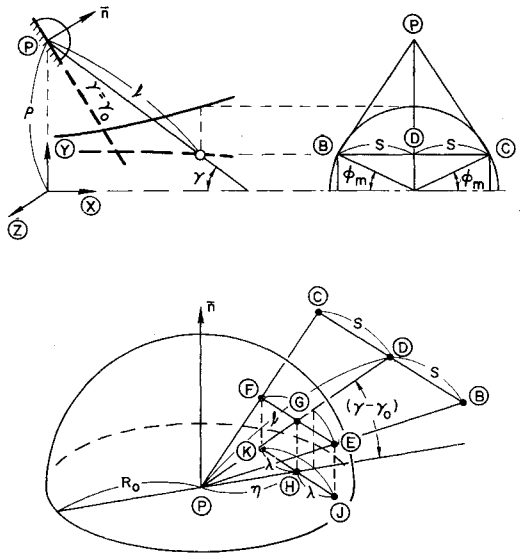

Fig. 2 Double projection of boundary points on hemispherical base.

Received May 7, 1964; revision received July 2, 1964.
* Member of Technical Staff. Member AIAA.

arc segment KJ is integrated over the same range of γ and if the areas of elliptical segments bounded by the arc segment KJ and the line segment KJ for the two limiting angles are added or subtracted, the same projected area will result. The latter approach is used herein. The integrated area of the line segment is denoted by ΔA. The area of an elliptical segment should be added if the arc segment lies outside of the integrated area and subtracted if it lies inside.

The area of an elliptical segment for an angle γ is determined by

$$A_e = R_0^2 \cos(\gamma_0 - \gamma)\left\{\sin^{-1}\frac{(S/l)}{[1+(S/l)^2]^{1/2}} - \frac{(S/l)}{[1+(S/l)^2]}\right\} \tag{8}$$

where the value of (S/l) corresponds to the value of x for a given γ.

B. Shape factor to conical surface

For a conical surface, the equations derived in the preceding section can be simplified by the following substitution:

$$\mu = a\tan\theta_c \qquad \nu = \tan\theta_c \qquad \xi = 0$$

$$\left(\frac{S}{l}\right) = \frac{[(a/\rho)\sin\gamma + \cos\gamma]\tan\theta_c}{[1-(a/\rho)^2\tan^2\theta_c]^{1/2}} \tag{9}$$

where a is the distance from the cone vertex to the origin, and θ_c is a half-cone angle.

C. Shape factor to cylindrical surface

For a cylindrical surface, further simplification of the equation is possible by following substitution:

$$\mu = R_c \qquad \nu = \xi = 0$$

$$\left(\frac{S}{l}\right) = \frac{(R_c/\rho)\sin\gamma}{[1-(R_c/\rho)^2]^{1/2}} \tag{10}$$

where R_c is the radius of a cylinder. It should be noted that for the conical and cylindrical cases, the value of (S/l) is computed directly as a function of γ. However, for the quadratic case, the values of (S/l) and γ must be computed as functions of x.

D. Blockage effects

In some cases, the surface element is located such that its view from an axisymmetric surface is blocked by another surface such as nozzle wall. In such cases, the projected area of the blockage must be subtracted from the total projected area of the surface.

As seen from Fig. 3, if $\gamma_0 > \gamma_{N_2}$, the blocking exists. The following geometric relations are obtained from Fig. 3:

$$\tan\gamma_{N_1} = \frac{1-(R_N/\rho)\sin\phi_m\,(\text{at } x=\delta)}{(\delta/\rho)} \tag{11}$$

$$\tan\gamma_{N_2} = \frac{(\rho - R_N)}{\delta} \tag{12}$$

$$\left(\frac{S_N}{l_N}\right) = \frac{\cos\gamma}{(\delta/\rho)}\cdot\left\{\left(\frac{R_N}{\rho}\right)^2 - \left[1-\left(\frac{\delta}{\rho}\right)\tan\gamma\right]^2\right\}^{1/2} \tag{13}$$

If $\gamma_0 \geq \gamma_{N_1}$, the computation starts from $\gamma = \gamma_{N_1}$. However, if $\gamma_{N_1} > \gamma_0 > \gamma_{N_2}$, it starts from $\gamma = \gamma_0$.

III. Computational Method

Presented herein is the computational procedure for determining the shape factor between a surface element and an axisymmetric surface by use of the foregoing analytical solutions. For convenience, the radius of the hemisphere R_0 is taken to be unity.

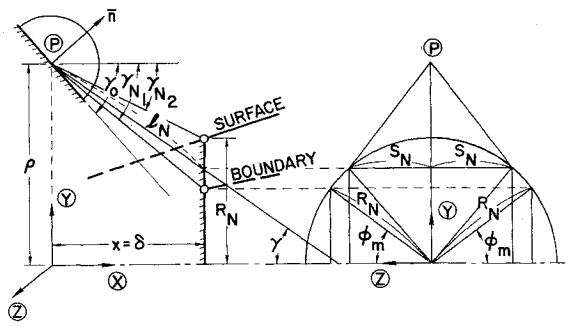

Fig. 3 Shading of axisymmetric surface.

A. Integrated area (ΔA) between two limiting angles

1) Check the condition for the existence of blockage effect. If "no," use $\gamma_i = \gamma_0$. If "yes" and if $\gamma_0 \leq \gamma_{N_1}$, use $\gamma_i = \gamma_0$. If "yes" and if $\gamma_0 > \gamma_{N_1}$, use $\gamma_i = \gamma_{N_1}$.

2) For the conical and cylindrical cases, compute (S/l), λ, and η as functions of γ between the initial angle γ_i and the final angle γ_f. For quadratic case, compute γ, (S/l), λ, and η as functions of x between x_i and x_f, corresponding to γ_i, and γ_f, respectively.

3) Determine the area under the λ-η curve and double it to obtain ΔA.

B. Area of elliptical segment (A_e)

The area of an elliptical segment can be determined directly from Eq. (8).

C. Area due to blockage (A_N)

1) Compute (S_N/l_N), λ, and η for γ between γ_i and γ_{N_2} by using Eqs. (13, 6, and 7), respectively.

2) Determine the area under the λ-η curve and double it to obtain A_N.

D. Shape factor

The shape factor can be determined by simply combining these areas and dividing by π.

1) For the shape factor without blockage effect,

$$F = (1/\pi)[\Delta A \pm A_e(\gamma_i) \pm A_e(\gamma_f)] \tag{14}$$

2) For the shape factor with blockage effect,

$$F = (1/\pi)[\Delta A - A_N \pm A_e(\gamma_f)] \tag{15}$$

The areas $A_e(\gamma_i)$ and $A_e(\gamma_f)$ are added or subtracted in the foregoing equations depending upon whether these segments lie outside or inside the area ΔA.

IV. Limitations of the Technique

It is seen from Eq. (2b) that the value of $\sin\phi_m$ can become greater than 1 or less than -1. The former implies that the surface element lies inside the surface, which is physically impossible. The latter implies that the element sees the entire surface. The foregoing technique, therefore, cannot be applied to this particular case. For $\gamma_0 = 90$, the solution of Ref. 1 for configuration P-6 may be used.

The analysis presented here is based on the assumption that the normal vector of a surface element always lies in the x-y plane. If the normal vector is not in this plane, other methods of solution must be used. Suppose that the projection of the normal vector on the x-z plane makes an angle β with the x axis. If this angle is small, then the shape factor can be estimated by simply multiplying the shape factor computed for $\beta = 0$ by the factor

$$\psi = [1 - (\sin\gamma_0 \sin\beta)^2]^{1/2}$$

V. Conclusion

In the technique described here, a numerical method for determining the projected areas has been used. For the

conical case, the analytical solutions are also available in Ref. 2. The technique presented herein can be applied to an axisymmetric surface of infinite length as well as that of finite length. It can also be applied to the segmentation of a surface in case the shape factor variation with longitudinal distance is desired.

References

[1] Hamilton, D. C. and Morgan, W. R., "Radiant-interchange configuration factors," NACA TN2836, Purdue Univ. (December 1952).

[2] Morizumi, S. J., "Analytical method of determining shape factor from a surface element to a conical surface," Space Technology Labs. Internal Memo. 62-9721. 4-78 (October 1962).

Effect of Boundary-Layer Removal on High Velocity Flame Stabilization

JAMES R. MAUS*
North Carolina State College, Raleigh, N. C.
AND
WILLIAM T. SNYDER†
State University of New York, Stony Brook, N. Y.

THE present investigation is concerned with the influence of the boundary-layer structure, as exemplified by the measured velocity profiles and boundary-layer mass flow rate, on flame stabilization utilizing the recessed wall flame holder. The feasibility of recessed wall stabilization has been demonstrated,[2] and a qualitative investigation of the influence of boundary-layer thickness on flame stabilization with the recessed wall flame holder has been reported.[4]

The impetus for the present investigation was the studies by Cheng and Kovitz[1] and Marble and Adamson[3] on mixing and ignition of a combustible mixture in the laminar wake of a flat plate. The Marble and Adamson investigation considered both streams to have initially uniform velocity profiles, whereas the Cheng and Kovitz analysis considered the effect of initial velocity distributions in the two streams. It was found that the inclusion of nonuniform initial velocity boundary layers affects considerably the temperature and concentration profiles downstream of the initial contact point.

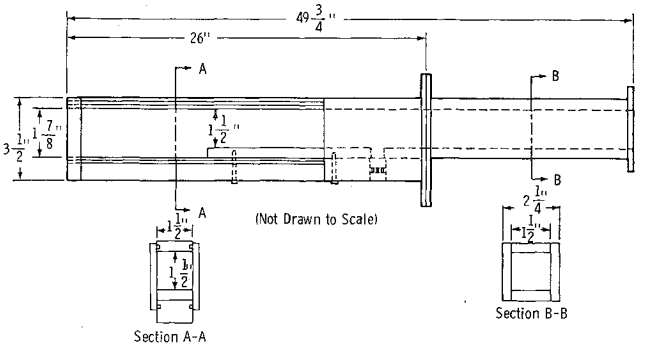

Fig. 1 Detail of test section.

Received June 19, 1964. The authors gratefully acknowledge the financial assistance of the National Science Foundation through Grant No. G-10355 which made this investigation possible.

* Ford Foundation Fellow.

† Associate Professor of Engineering; now at University of Tennessee Space Institute, Arnold Air Force Station, Tenn.

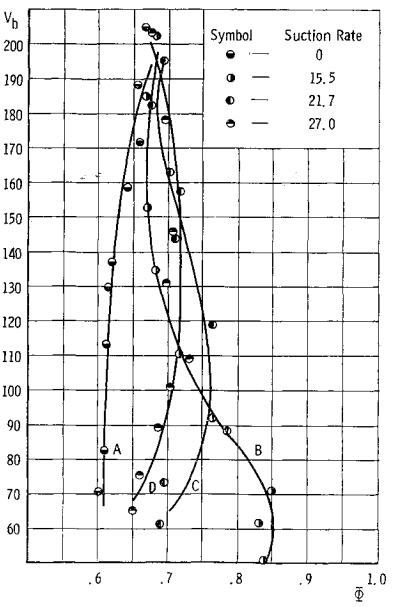

Fig. 2 Blowoff curves: *A*, no suction; *B*, suction rate of 15.5 standard ft³/min; *C*, suction rate of 21.7 standard ft³/min; and *D*, suction rate of 27.0 standard ft³/min.

In the present investigation, the flame stabilizer is the recessed wall and the mixture is a premixed, homogeneous mixture of air and propane. A suction slot of variable width is provided upstream of the point of stabilization, and the boundary-layer structure at the point of stabilization is varied by boundary-layer suction through the suction slot. The suction flow is metered, and the geometry of the apparatus is shown in Fig. 1.

Velocity profiles were measured in the cold flow boundary layer at the stabilization point using a flow corporation model HWB2 hot wire anemometer and a 0.00035-in. tungsten wire. Velocity profiles and blowout curves were obtained without suction, and blowout curves were obtained with three different suction rates. The lean blowoff curves with and without suction are shown in Fig. 2.

From the measured velocity profiles, the boundary-layer mass flow rate without suction was calculated by graphical integration of the velocity profiles. Knowing the boundary-layer flow without suction, the suction rate was then normalized by defining a parameter R as the ratio of the suction flow rate to the boundary-layer flow rate at the flame holder in the absence of suction. The lean blowoff data of Fig. 2 could then be correlated by plotting $\Phi s/\Phi 0$ against R with velocity as the parameter where $\Phi s/\Phi 0$ is the ratio of the equivalence ratio at blowoff with suction to that at blowoff without suction at the same value of blowoff velocity (taken as the mean velocity of the cold flow preceding the point of stabilization). This correlation is shown in Fig. 3.

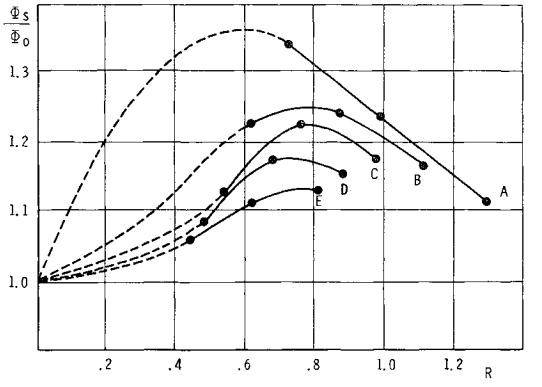

Fig. 3 Quotient of equivalence ratios with and without suction vs ratio of suction rate to boundary-layer flow. *A*, V_b = 80 fps; *B*, V_b = 100; *C*, V_b = 120; *D*, V_b = 140; and *E*, V_b = 160.